RSC Advances

REVIEW

View Article Online
View Journal | View Issue

Cite this: *RSC Adv.*, 2025, **15**, 19088

Advances in Co_3O_4 nanomaterial-based photocatalysts for water purification: mechanisms, green synthesis, activation of oxidants, waste-derived sources, and computational insights

Van Dien Dang,[a] Nguyen Thi Hong Nhung,[b] Iqra Rabani,[c] Nguyen Tien Tran,[de] Bui Thi Phuong Thuy [f] and Hai Bang Truong [*gh]

Received 17th April 2025
Accepted 20th May 2025

DOI: 10.1039/d5ra02705e

rsc.li/rsc-advances

Water scarcity remains a critical global challenge, affecting billions of people and significantly impacting ecosystems, economies, and public health. Among various water treatment technologies, photocatalysis has emerged as a highly effective method for degrading a wide range of contaminants. Cobalt oxide (Co_3O_4) has gained considerable attention as a photocatalyst due to its unique structural, electronic, and optical properties. Despite extensive research on the synthesis and application of Co_3O_4-based photocatalysts, a comprehensive review summarizing recent advancements and modifications in Co_3O_4 nanomaterials over the past five years is notably lacking. This review critically examines the fundamental photocatalytic mechanisms of Co_3O_4 nanomaterial-based systems, systematically discussing their advantages and inherent limitations. Additionally, it explores emerging research trends, including biosynthesis, facile recovery, synthesis from waste-derived sources, and computational techniques, alongside the prevailing challenges shaping this field. Furthermore, the review identifies key research directions for the future development and optimization of Co_3O_4-based nanostructures, emphasizing

[a]*Faculty of Biology and Environment, Ho Chi Minh City University of Industry and Trade, 140 Le Trong Tan, Tan Phu District, Ho Chi Minh 700000, Vietnam*
[b]*Faculty of Applied Science and Technology (FAST), Nguyen Tat Thanh University, 331 National Highway 1A, An Phu Dong Ward, District 12, Ho Chi Minh City 700000, Vietnam*
[c]*Antwerp Engineering, Photoelectrochemistry and Sensing (A-PECS), University of Antwerp, Groenenborgerlaan 171, 2020 Antwerp, Belgium*
[d]*Center for Advanced Chemistry, Institute of Research and Development, Duy Tan University, Da Nang 550000, Vietnam*
[e]*Faculty of Natural Sciences, Duy Tan University, Da Nang 550000, Vietnam*
[f]*Faculty of Fundamental Sciences, Van Lang University, Ho Chi Minh City, Vietnam*
[g]*Optical Materials Research Group, Science and Technology Advanced Institute, Van Lang University, Ho Chi Minh City, Vietnam*
[h]*Faculty of Applied Technology, School of Technology, Van Lang University, Ho Chi Minh City, Vietnam. E-mail: truonghaibang@vlu.edu.vn*

Van Dien Dang

Van Dien Dang, PhD, received his doctoral degree in Environmental Science and Technology from National Yang Ming Chiao Tung University, Taiwan. He is currently a lecturer at Ho Chi Minh City University of Industry and Trade, Vietnam. His research focuses on nanomaterials for environmental remediation and energy storage/production, including photocatalysis, supercapacitors, syngas pyrolysis, and electrocatalytic hydrogen evolution. Dr Dang has published over 25 papers in Q1 journals related to environmental science.

Nguyen Thi Hong Nhung

Nguyen Thi HongNhung is a dedicated lecturer and researcher at Nguyen Tat Thanh University, Vietnam, specializing in the application of technology for waste management and environmental protection. Currently pursuing a PhD in Resource and Environmental Management, she is actively engaged in academic publishing with a focus on ISI and Scopus-indexed journals.

their potential to enhance photocatalytic efficiency for water purification. By addressing these aspects, this work aims to bridge existing knowledge gaps and provide a foundation for future innovations in sustainable water treatment technologies.

1. Introduction

Water scarcity is a severe global issue affecting billions of people and posing significant challenges to ecosystems, economies, and public health. According to UNESCO, the number of urban residents facing water scarcity is expected to reach 2.5 billion by 2050.[1] Thus, potential solutions for effective water treatment and reusability are urgently required to promote more sustainable and livable futures. Among the water treatment methods, photocatalysis offers distinct advantages in efficiently degrading a wide spectrum of pollutants.[2,3] This eco-friendly process minimizes byproducts, utilizes renewable solar energy, and reduces chemical and energy demands.[4] Cost-effective and operable under ambient conditions, photocatalysis is scalable and versatile, suitable for applications from small systems to large-scale plants.[5] Compared to chlorination or reverse osmosis, it is more sustainable, less dependent on chemicals, and particularly effective against emerging contaminants.[6] Photocatalysis involves a series of interconnected processes.[7] It begins with light absorption, followed by the separation of electrons and holes. These charge carriers then migrate to the photocatalyst's surface, where active species are formed and conduct the reduction and oxidation reactions. At its core, photocatalysis utilizes optical energy to activate

Iqra Rabani

Dr. Iqra Rabani received her PhD degree in 2022 from Sejong University, South Korea. Following her doctoral studies, she served as an assistant professor for 32 months in the Department of Nanotechnology and Advanced Materials at Sejong University. Currently, she is a Marie Curie Postdoctoral Fellow at the University of Antwerp, Belgium. Her research focuses on eco-friendly organic–inorganic hybrid materials for cosmetics and wastewater treatment. She specializes in wearable energy storage and sustainable energy solutions. Her work bridges material science and applied nanotechnology, contributing to innovations in environmental sustainability and next-generation energy technologies.

Bui Thi Phuong Thuy

Bui Thi Phuong Thuy, PhD, is a dedicated lecturer and researcher at Van Lang University, Vietnam. With a strong background in theoretical and physical chemistry, she focuses on applied research in natural product extraction, pharmaceutical chemistry, and environmental applications. Formerly a faculty member at Dong Nai Technology University (2014–2019), Dr Thuy is actively engaged in academic publishing, targeting Q1, ISI, and Scopus-indexed journals.

Nguyen Tien Tran

Nguyen Tien Tran, PhD, received his doctoral degree in chemical engineering from Kyung Hee University, South Korea, in 2019. He is currently a research scientist in the Center for Advanced Chemistry at the Institute of Research and Development (IRD), Duy Tan University, Viet Nam. His current research interests include the synthesis of nanomaterials and their application, focusing on catalysts, adsorption, sensors, gas storage and separation, the development of numerical methodology, the dynamics of high-speed forming of material structures, and creating new materials.

Hai Bang Truong

Dr. Truong Hai Bang received his PhD degree in Engineering and Environmental Science from Sejong University, South Korea, in 2021. He previously worked as a postdoctoral researcher in the DOM Lab at Sejong University for 1.5 years. He is currently a research scientist at Van Lang University, Vietnam. His research focuses on environmental remediation technologies, including photocatalysis, membrane filtration, adsorption, advanced oxidation processes, and computational applications. Dr Truong Hai Bang has published over 60 ISI-indexed papers, 45 of which are in Q1 journals.

catalysts, producing reactive oxygen species with strong oxidative properties capable of degrading water contaminants.[8]

Cobalt oxide (Co_3O_4) is a promising photocatalytic material due to its distinctive structural, electronic, and optical features.[9] As a p-type semiconductor with a spinel configuration, Co_3O_4 exhibits excellent redox activity, facilitated by its mixed oxidation states (Co^{2+} and Co^{3+}). Its narrow bandgap (1.5–2.4 eV) enables visible light absorption, crucial for solar energy-driven photocatalysis.[10] Co_3O_4 is cost-effective, easy to synthesize, environmentally compatible, and offers excellent chemical stability and reversible redox performance.[11] However, its performance is limited by charge recombination, photocorrosion under prolonged light exposure, and structural degradation in harsh environments.[10] The bulk form of Co_3O_4 often exhibits limited surface area, restricting the quantity of active sites and further diminishing photocatalytic activity.[12] Despite cobalt's relative abundance, the scalability and economic viability of large-scale Co_3O_4 production remain challenges for broader application in photocatalysis.

The preparation of materials at the nanoscale has emerged as a prominent strategy in recent years to significantly enhance the efficiency and versatility of photocatalysis.[13] Nanostructures, including nanoparticles, nanorods, nanosheets, and nanotubes, exhibit a high surface-to-volume ratio, thereby increasing the quantity of active sites available for pollutant adsorption and catalytic reactions, which in turn improves overall photocatalytic performance.[6,14] Additionally, the dimension, shape, and composition of nanomaterials can be precisely tailored to modulate their electronic properties, such as the bandgap, thereby enabling the absorption of a broader spectrum of solar radiation.[15] Doping these nanomaterials with metals, non-metals, or engineering heterojunctions with other semiconductors further enhances charge carrier separation, mitigating electron–hole recombination and optimizing photocatalytic efficiency.[16]

Despite extensive research on the synthesis and application of Co_3O_4-based photocatalysts, there remains a notable paucity of review articles addressing the advancements and modifications in Co_3O_4-based nanomaterial systems in the recent five years for the efficient decomposition of pollutants in water. This review provides a critical assessment of the underlying photocatalytic mechanisms, delineating the advantages and limitations inherent to these systems. In addition, it offers an in-depth analysis of the prevailing research trends, including biosynthesis, facile recovery, synthesis from waste-derived sources, photocatalytic activation of oxidants, and computational techniques, alongside the prevailing challenges shaping this field. Finally, the review outlines prospective research trajectories for the development and optimization of Co_3O_4 nanostructures in the photocatalytic remediation of contaminated water, emphasizing key areas of significant potential for future exploration.

2. Physical and chemical characteristics of Co_3O_4

Co_3O_4 is a mixed-valence transition metal oxide that crystallizes in a spinel structure, where Co^{2+} ions occupy tetrahedral sites and Co^{3+} ions are located in octahedral positions within a close-packed oxygen lattice.[17] This distinctive arrangement confers Co_3O_4 with remarkable redox flexibility and facilitates efficient electron transfer and oxygen mobility, which are essential for photocatalytic activity. As a p-type semiconductor, Co_3O_4 exhibits a relatively narrow band gap in the range of 1.4 to 2.2 eV,[18,19] enabling strong absorption in the visible region of the electromagnetic spectrum. The valence band is composed of O 2p orbitals, while Co 3d orbitals form the conduction band, allowing effective excitation of electron–hole pairs under solar illumination.[20] This optical behavior makes Co_3O_4 highly attractive for sustainable photocatalytic water treatment, particularly in solar-driven pollutant degradation processes. One of the standout advantages of Co_3O_4 is its robust thermal and chemical stability. The material retains its crystalline structure at temperatures exceeding 800 °C and remains stable across a wide pH spectrum.[21,22] This durability ensures reliable long-term performance, particularly in harsh or variable water treatment environments. Although cobalt exists naturally in various minerals such as cobaltite, erythrite, and heterogenite, Co_3O_4 used in photocatalysis is typically produced through synthetic processes to ensure purity, controlled morphology, and reproducible performance.[23] These laboratory-based preparations are necessary to generate nanoscale Co_3O_4 with tailored surface area, crystal facets, and defect densities, which are not easily obtained from naturally occurring sources.[24] Compared to many conventional materials, this level of tunability greatly enhances Co_3O_4's catalytic performance and practical utility. The photocatalytic performance of Co_3O_4 is heavily influenced by its physicochemical features, which are governed by the synthesis method. A wide range of fabrication techniques have been developed to engineer Co_3O_4 nanostructures with desirable morphology and crystallinity.[25] Tailored nanostructures not only increase the surface-to-volume ratio but also introduce oxygen vacancies and unsaturated cobalt sites that act as active centers for photocatalytic reactions. The surface defects enhance visible-light absorption and promote the formation of reactive oxygen species, such as hydroxyl and superoxide radicals, which are pivotal in decomposing organic contaminants. Building upon the crucial role of surface structure and defects, the following section reveals deeper into how different synthesis routes shape the morphology of Co_3O_4 nanomaterials and influence their photocatalytic behavior.

3. Synthesis and morphology of Co_3O_4 nanomaterial-based photocatalysts

The morphology of Co_3O_4 nanomaterials plays a pivotal role in governing their photocatalytic efficacy, as it influences key factors such as light absorption, charge separation, surface reactivity, and the availability of active sites. Among the various Co_3O_4 nanostructures, nanospheres are the most prevalent due to their versatile synthesis methods, including hydrothermal, solvothermal, co-precipitation, calcination, and

biosynthesis.[26–31] The diameters and band gap energies of Co_3O_4 nanospheres exhibit a wide range, spanning from 6 to 100 nm and 1.77 to 3.86 eV, respectively, which significantly impacts their photocatalytic performance. Different from most recent studies that synthesize Co_3O_4 from synthetic chemical precursors, Dhiman and Gupta successfully synthesized Co_3O_4 nanoparticles from discarded batteries for photocatalytic decomposition of methylene blue dye[32] (Table 1). In their approach, various solutions, including Cyphos IL 102, HCl, and oxalic acid, were employed to extract cobalt from a mixture of metals. Co_3O_4 nanoparticles were subsequently formed *via* a calcination process, demonstrating the ability to completely degrade 50 mg L^{-1} of MB within 3 hours of solar light exposure. While this study presents a promising approach to converting hazardous waste into a material for environmental remediation, further investigations are necessary to fully elucidate the electronic, optical, and photocatalytic features of the as-synthesized Co_3O_4 nanomaterials.

For alternative morphologies, J. Yang *et al.* employed rose petal as a template to fabricate Co_3O_4 nanosheets with an ultrathin structure (~0.1 μm) through calcination method[33] (Fig. 1a). The Co_3O_4 nanosheets exhibited a porous architecture with an increased surface area (52 m^2 g^{-1}), which facilitated enhanced charge transport and increased methylene blue dye adsorption, thereby promoting effective photocatalytic degradation. However, the photocatalytic mechanism underlying methylene blue degradation was not thoroughly elucidated, as the study did not measure the energy band structure of Co_3O_4 nor the generation of active species during the process. Co_3O_4 mesoporous have garnered significant notice in recent research due to their inherent advantages, including large surface areas, highly accessible active sites, enhanced diffusion of pollutants into the material and degradation products out of it, and improved stability of nanoparticles by preventing sintering during photocatalytic reactions. For instance, mesoporous Co_3O_4 nanoparticles were synthesized *via* sol–gel technique, utilising the soft template F-127, for the photocatalytic degradation of the tetracycline antibiotics[34] (Fig. 1b). The Co_3O_4 exhibited a large surface area (S_{BET} = 178 m^2 g^{-1}) with an average pore diameter of 8 nm, which facilitated the efficient transport and penetration of antibiotic molecules to the active sites. Under optimized conditions, at a dosage of 1 g L^{-1}, the Co_3O_4 photocatalyst achieved 66% degradation of tetracycline (20 mg L^{-1}) within 1.5 hours of light irradiation.

Table 1 Typical studies on Co_3O_4 nanomaterial-based photocatalysts with varied morphologies in the application for water treatment

System (dose)	Synthesis method & light source	Pollutant (concentration)	Removal efficiency (irradiation time)	Ref.
Nanoparticle Co_3O_4 (0.25 g L^{-1})	Extraction of cobalt from waste batteries using Cyphos IL 102 and calcination (600 °C) Solar light[a]	Methylene blue (50 mg L^{-1})	UV-VIS: 100% (180 min)	32
Nanosheet Co_3O_4 (0.6 g L^{-1})	Calcination with rose petal as template (550 °C) Xenon lamp[a]	Methylene blue (10 mg L^{-1})	UV-VIS: 92% (60 min)	33
Mesoporous nanoparticles Co_3O_4 (1 g L^{-1})	Sol–gel with soft template and calcination (650 °C) Xenon lamp (300 W)	Tetracycline (20 mg L^{-1})	UV-VIS: 66% (105 min)	34
Quantum dot Co_3O_4 (0.3 g L^{-1})	Solvothermal (80 °C) & mixing Xenon lamp (150 W)	Tetracycline (20 mg L^{-1})	UV-VIS: 33% (80 min)	35
Nanocage cube Co_3O_4 (0.8 g L^{-1})	Calcination from ZIF-67 (500 °C) LED lamp (1 W)	Tetracycline (30 mg L^{-1})	UV-VIS: 14% (240 min)	36
Polyhedral nanoparticle Co_3O_4	Calcination from ZIF-67 (300 °C) Xenon lamp (150 W)	Norfloxacin (20 mg L^{-1})	UV-VIS: 38% (90 min)	37
Spherical Co_3O_4 (0.2 g L^{-1})	Green synthesis using *Piper betle* extract and calcination (600 °C) 6 UV-lamp (6 W)	Eriochrome T (60 mg L^{-1})	UV-VIS: 94% (80 min)	26
Nanoparticle Co_3O_4 (1 g L^{-1})	Green synthesis using *Aloe barbadensis* and calcination (900 °C) Sunlight[a]	Rhodamine B (10 mg L^{-1})	UV-VIS: 97% (255 min)	27
Nanoparticle SF-Co_3O_4 (100 g L^{-1})	Green synthesis using sunflower seeds (500 °C)	Methylene blue	UV-VIS: 90% (120 min)	38
Nanoparticle GC-Co_3O_4 (100 g L^{-1})	Green synthesis using green chilli (500 °C) Xenon lamp (150 W)		UV-VIS: 70% (120 min)	

[a] Light intensity is not reported in the referenced literature.

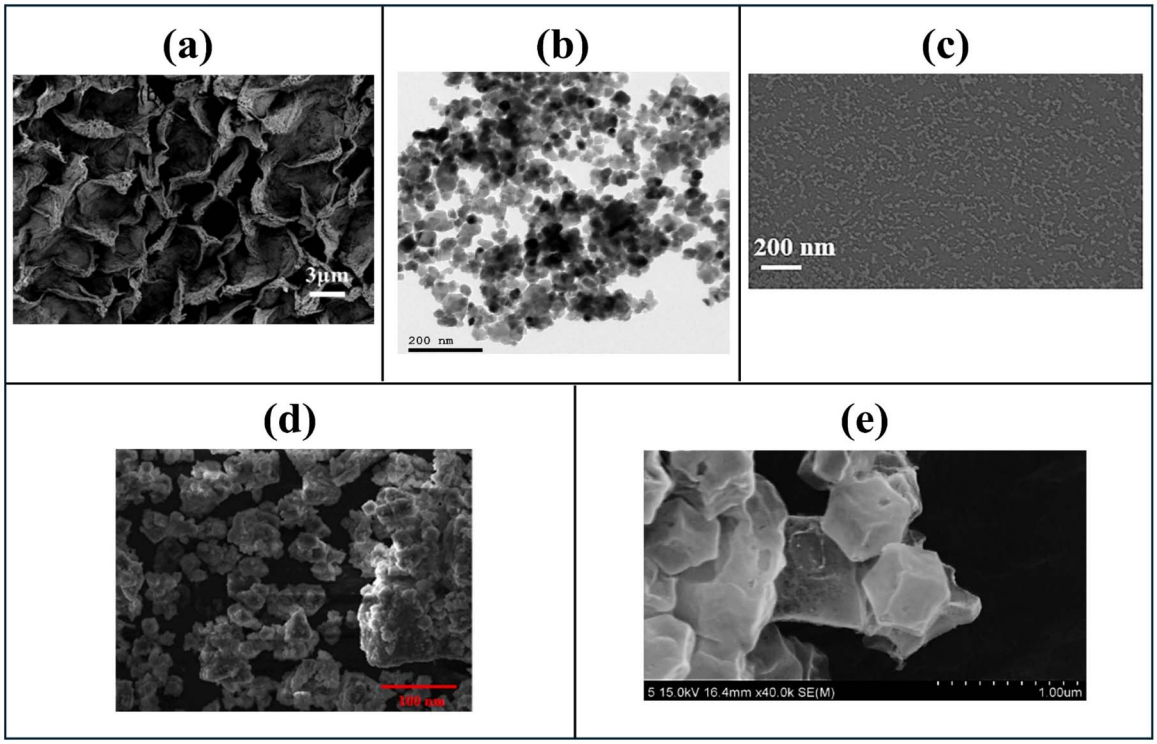

Fig. 1 Co_3O_4 nanomaterial-based photocatalysts with varied morphologies in the application for water treatment in the recent five years: nanosheet Co_3O_4 (ref. 33) (a), mesoporous Co_3O_4 (ref. 34) (b), quantum dot Co_3O_4 (ref. 35) (c), polyhedral Co_3O_4 (ref. 38) (d), and cubic Co_3O_4 (ref. 37) (e). Reprinted with permission from ref. 33 Copyright (2019), ref. 34 Copyright (2023), ref. 35 Copyright (2022), ref. 38 Copyright (2022), and ref. 37 Copyright (2024), with permission from Elsevier.

Nanosized Co_3O_4 quantum dots exhibit several advantageous properties, including a short charge transfer path, enhanced photostability, broad light absorbance, and a quantum confinement effect, all of which contribute to improved electron–hole pair generation and separation, thereby enhancing catalytic efficiency. Additionally, Co_3O_4 quantum dots can be uniformly dispersed in solvents such as water or ethanol, facilitating their easy incorporation onto the surface of photocatalysts *via* a temperature-dependent deposition process. In a representative study, Zhang *et al.* prepared Co_3O_4 quantum dots by solvothermal methods for the photocatalytic treatment of tetracycline[35] (Fig. 1c). The individual Co_3O_4 quantum dots demonstrated limited photocatalytic activity under visible light illumination (33% of tetracycline degradation in 80 min of light exposure). Although quantum dots can absorb a wide range of light, their small size (3–5 nm) led to rapid charge carrier recombination and poor stability under prolonged exposure to pollutants. Moreover, the high surface-to-volume ratio of the Co_3O_4 quantum dots resulted in the creation of surface trap states. These traps can capture charge carriers and prevent them from contributing to photocatalytic reactions, which reduces the overall photocatalytic efficiency. Consequently, it is often recommended to combine Co_3O_4 in quantum dot structure with another semiconductor to form composite materials, thereby creating additional charge transfer pathways and facilitating the effective generation of active species.

The synthesis of Co_3O_4 nanomaterials from cobalt-based metal–organic framework (MOF) precursors, particularly ZIF-67, has emerged as a prominent research focus in recent years. Co_3O_4-based MOFs integrate the distinctive physicochemical properties of both MOFs and Co_3O_4 contributing to enhanced photocatalytic effectiveness. Specifically, MOF structures contain hollow cavities that facilitate multiple reflections and refractions of absorbed light, thereby prolonging its residence time and increasing the generation of photoexcited electron–hole pairs. Imanuella *et al.* successfully synthesized Co_3O_4 nanocages with a cubic morphology by calcining ZIF-67 at 500 °C.[36] However, the resulting Co_3O_4 exhibited relatively low photocatalytic performance, achieving only 14% degradation of tetracycline (30 mg L^{-1}) after six hours of simulated solar irradiation. Nevertheless, when incorporated into a composite system with CdS, the Co_3O_4 nanocage facilitated charge separation through the formation of an F-scheme heterojunction, significantly enhancing tetracycline removal to 83%. In another study, Adhikari *et al.* synthesized polyhedral Co_3O_4 nanoparticles by calcining ZIF-67 at 300 °C[38] (Fig. 1d). The material demonstrated moderate photocatalytic activity, decomposing 38% of norfloxacin under 90 minutes of visible-light exposure. Furthermore, the Co_3O_4 nanoparticles were reported to form a p–n heterojunction with MoS_2, exhibiting a type-II band alignment that significantly improved the migration rates of photoexcited charge carriers, thereby enhancing overall photocatalytic performance.

It was noticed from the studies above that the morphology of Co_3O_4 nanomaterial-based photocatalysts significantly influences their light-harvesting efficiency, charge dynamics, and catalytic reactivity. Controlled morphological engineering, including the development of hierarchical, porous, and composite structures, is crucial for optimizing performance in environmental and energy applications. Porous and hollow Co_3O_4 nanostructures improve photocatalytic efficiency by increasing surface area and active site availability, while mesoporous and macroporous frameworks improve reactant diffusion and reaction kinetics. Morphologies designed to trap light, such as hierarchical and porous configurations, enhance photon absorption, and nanostructures with tunable dimensions, like quantum dots, enable bandgap optimization for broader solar spectrum utilization. Additionally, core–shell and layered morphologies of Co_3O_4 nanomaterials improve durability by mitigating photocorrosion and structural degradation under operational conditions.

4. Biosynthesis of Co_3O_4 nanomaterial-based photocatalysts

The biosynthesis of nanomaterials has attracted lots of attention in recent research due to its sustainability and efficiency. This biologically driven approach employs microorganisms and plants as natural nanofactories, obviating the need for hazardous chemicals. Moreover, biosynthesis occurs under ambient temperature and pressure conditions while utilizing renewable or waste-derived biomaterials, thereby enhancing its economic viability and energy efficiency.

The biosynthesis of nanomaterials generally follows two main mechanistic pathways. The first is the biochemical reduction mechanism, in which naturally occurring reducing agents convert metal ions into their zero-valent or oxide forms, initiating the nucleation and growth of nanocrystals. Several research groups have recently adopted this biochemical reduction mechanism in the green synthesis of Co_3O_4 nanomaterials for water purification applications (Table 1). Most Co_3O_4 nanomaterials synthesized *via* the biochemical reduction pathway exhibit spherical or quasi-spherical morphologies. In 2022, S. Kumar *et al.* successfully synthesized spherical Co_3O_4 nanoparticles using *Piper betle* extract, achieving a yield ratio of 4 : 1 (Co_3O_4 : extract)[26] (Fig. 2). The photocatalytic activity of the Co_3O_4 was comprehensively assessed through quantum yield, space-time yield, and figure-of-merit calculations. At an optimal concentration of 0.2 g L^{-1}, the material demonstrated 94% breakdown of Eriochrome T dye (60 mg L^{-1}) within 80 minutes. Although Co_3O_4 exhibits a high band gap energy (3.86 eV), defect states such as oxygen and cobalt vacancies or interstitials enable charge carrier excitation under solar or visible light. The study did not verify the photocatalytic generation and mechanistic roles of reactive oxygen species. Moreover, future research should aim to identify the key components in *P. betle* leaf extract in order to optimize the extraction process, selectively enrich active compounds, and maximize the yield and quality of Co_3O_4 nanoparticles. Sarvalkar *et al.* synthesized Co_3O_4 nanospheres with diameters ranging from 6 to 20 nm using an *Aloe barbadensis* extract-mediated green approach.[27] The biogenically derived Co_3O_4 was evaluated for the decomposition of rhodamine B under sunlight exposure. The system required an extended period of 24 hours in darkness to attain adsorption equilibrium between Co_3O_4 and the target dye. Additionally, the photocatalytic efficiency was relatively low, as a high catalyst loading of 1 g L^{-1} was necessary to achieve 97% degradation of 10 mg L^{-1} rhodamine B over 255 minutes. Furthermore, the study did not elucidate the photocatalytic mechanism, as it did not explore the electronic band structure or identify the reactive species responsible for the degradation process. The composition of *A. barbadensis* extract was not clarified to identify the key bioactive compounds involved in the reduction of metal ions to nanoparticles. In another study, Khalid *et al.* prepared two distinct Co_3O_4 nanomaterials using sunflower seed and chili extract for the photocatalytic removal of methylene blue dye.[38] Despite identical synthesis conditions, Co_3O_4 nanomaterials derived from different bio-extracts exhibited varied properties and photocatalytic performance. The Co_3O_4 nanoparticles derived from sunflower seed exhibited smaller particle size, a lower bandgap, and higher electrical conduction compared to those prepared using chili extract, resulting in superior photocatalytic performance for methylene blue degradation. These differences likely arise from the distinct bioactive compound compositions of each extract, which were not analyzed in the study. Noticeably, the high catalyst concentration required for the photocatalytic experiments (100 g L^{-1}) presents a significant cost limitation for practical applications. Additionally, the synthesized materials demonstrated bifunctional properties, exhibiting potential for both photocatalytic water treatment and electrochemical energy storage.

The second biosynthesis pathway involves capping or stabilization, in which biomolecules bind to the surface of forming nanomaterials to prevent agglomeration and regulate growth, thereby maintaining monodispersity and controlling their shape. In the study of Yang *et al.* (2019),[33] Co_3O_4 nanosheets were fabricated using a biotemplate derived from rose flower petals. The petal extract, rich in polysaccharides and proteins containing amine and carboxyl groups, formed complexes with Co^{2+} ions and inhibited their aggregation. As a result, cobalt ions were uniformly distributed on the petal surface and subsequently converted into Co_3O_4 nanosheets after calcination. These nanosheets exhibited significantly enhanced photocatalytic activity, degrading methylene blue three times faster than commercial Co_3O_4. The authors attributed this performance to the 2D porous structure, which facilitated electron migration from the bulk to the catalyst surface. However, the study did not investigate the generation of reactive species or elucidate the photocatalytic degradation mechanism.

The bandgap, structural morphology, and optical characteristics of Co_3O_4 nanomaterials synthesized *via* biological approaches are significantly influenced by the choice of biological precursors and the specific parameters governing the biosynthesis process. A critical analysis of existing studies indicates that a comprehensive understanding of the biomolecular interactions governing the synthesis of Co_3O_4

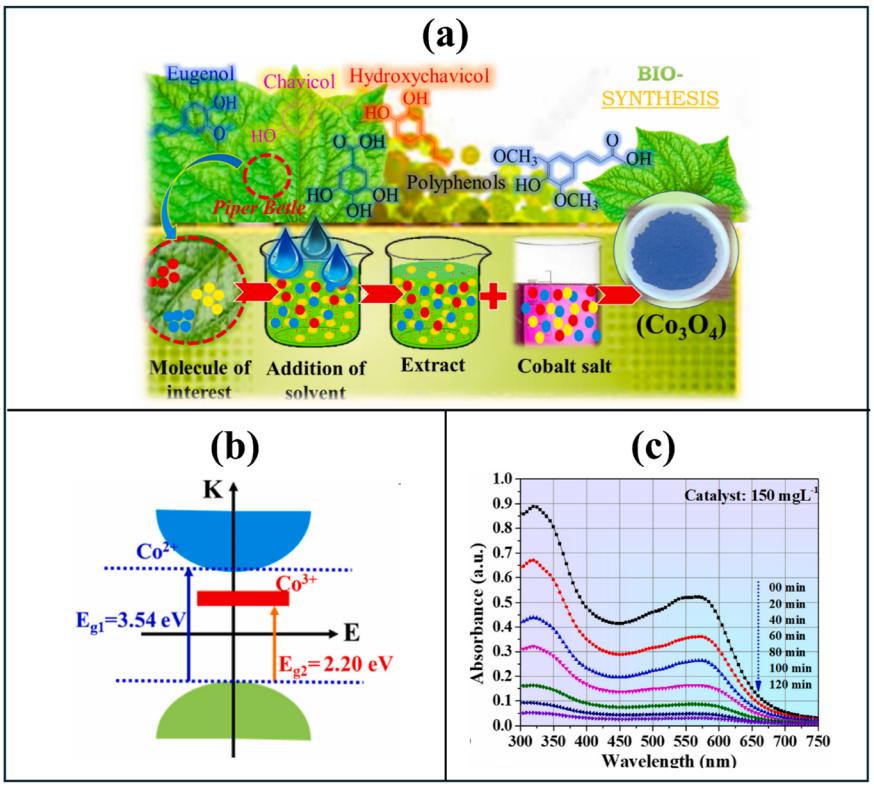

Fig. 2 Biosynthesis of Co_3O_4 nanoparticles from *Piper betle* extract[26] for photocatalytic degradation of Eriochrome Black T: synthesis process (a), electronic structure (b), and photocatalytic performance in degradation of Eriochrome Black T (c). Reprinted with permission from ref. 26, Copyright (2022), with permission from Elsevier.

nanoparticles remains largely unexplored. To address this gap, advanced spectroscopic and microscopic techniques should be employed to elucidate the precise roles of enzymes, proteins, and phytochemicals in the nucleation and growth processes of Co_3O_4 nanoparticles, which are fundamental for controlling their morphological and electronic properties.

Further research is required to evaluate the feasibility of diverse biological sources for Co_3O_4 synthesis to enhance the material's structural integrity and functional performance. Additionally, optimizing key synthesis parameters, such as annealing temperature, reaction pH, and the ratio of plant extract to Co_3O_4 precursor, is essential for achieving well-defined nanostructures with tailored physicochemical characteristics. Moreover, in-depth investigations into the reaction mechanisms, phase purity, and surface chemistry of biogenically synthesized Co_3O_4 are imperative to advance its potential applications, particularly in the photocatalytic remediation of contaminated water.

5. Photocatalytic systems with Co_3O_4 nanomaterials incorporated into other materials

5.1. Metal doping

Both metal doping and photocatalytic composite formation are extensively utilized approaches for improving the photocatalytic efficiency of materials. However, in recent years, research on the modification of Co_3O_4 through metal doping has been relatively limited, likely due to inherent challenges such as structural instability induced by lattice distortions and the tendency of doped nanomaterials to agglomerate or undergo uncontrolled growth, ultimately compromising their nanoscale features. In a study conducted by Keerthana *et al.* (2021), Sn was doped onto Co_3O_4 *via* the sol–gel and calcination method[39] for the treatment of methylene blue dye (Table 2). The 2% Sn-doped Co_3O_4 exhibited a methylene blue degradation efficiency of 75% within 180 minutes, representing only a 7% improvement over pristine Co_3O_4. This enhancement was attributed to the role of Sn doping in facilitating the growth of Co_3O_4 nanoparticles with reduced agglomeration and smaller particle size. The optimal Sn/Co_3O_4 sample maintained stable performance over three photocatalytic cycles. However, this limited testing, combined with the lack of post-reaction characterizations, prevents a thorough assessment of its long-term stability. Further investigations are necessary to elucidate the precise role of Sn doping and to comprehensively explore the photocatalytic mechanism governing dye degradation in Sn-doped Co_3O_4.

In another study, Mohamed *et al.* successfully modified mesoporous Co_3O_4 nanocrystals with PtO using the impregnation method.[40] The optimized 0.9% PtO-doped Co_3O_4 at a concentration of 1 g L^{-1}, achieved complete decomposition of 100 mg L^{-1} foron blue dye within one hour of visible-light irradiation, whereas unmodified Co_3O_4 nanoparticles degraded only 55% of the dye under the same conditions. The

Table 2 Summary on operational condition and photocatalytic performance of Co_3O_4 nanomaterial-based systems

Photocatalytic systems (dose)	Synthesis method/Light source	Pollutant (concentration)	Removal efficiency	Ref.
Metal-doped system				
Sn/Co_3O_4 (0.2 g L^{-1})	Sol–gel & calcination (400 °C) Light source: N/A	Methylene blue	UV-VIS: 75% (180 min)	39
PtO/Co_3O_4 (1 g L^{-1})	Sol–gel & impregnation Xenon lamp (500 W)	Foron blue (100 mg L^{-1})	UV-VIS: 100% (30 min)	40
Straddling type-I heterojunction composite				
$Bi_6Cr_2O_{15}/Co_3O_4$ (0.15 g L^{-1})	Sonochemical precipiation Halogen lamp (500 W)	Methylene blue (25 mg L^{-1})	UV-VIS: 91% (160 min)	41
Co_3O_4/TiO_2 (2 g L^{-1})	Impregnation using soft template Xenon lamp (300 W)	Ciprofloxacin (10 mg L^{-1})	UV-VIS: 100% (60 min)	42
rGO-Co_3O_4/ZnO (dose: N/A)	Two-step hydrothermal Light source: N/A	Parathion (25 mg L^{-1})	UV-VIS: 99.6% (140 min)	28
Bi_2O_3/BN/Co_3O_4 (1 g L^{-1})	Calcination & impregnation Xenon lamp (500 W)	Norfloxacin (5 mg L^{-1})	HPLC: 98% (180 min)	29
Type-II heterojunction composite				
$Co_3O_{4(QDs)}/Bi_2WO_6$ (0.3 g L^{-1})	Solvothermal & mixing Xenon lamp (300 W)	Tetracycline (20 mg L^{-1})	UV-VIS: 80% (20 min)	35
Red P/Co_3O_4 (0.4 g L^{-1})	Hydrothermal and physical mixing Xenon lamp (300 W)	Malachite green (20 mg L^{-1})	UV-VIS: 94% (20 min)	43
S-scheme composite				
Li_2MnO_3/Co_3O_4 (1 g L^{-1})	Sol–gel with soft template Xenon lamp (300 W)	Tetracycline (25 mg L^{-1})	UV-VIS: 100% (120 min)	44
$CuCo_2O_4/Co_3O_4$ (1 g L^{-1})	Sol–gel with soft template Xenon lamp (300 W)	Tetracycline (20 mg L^{-1})	UV-VIS: 100% (90 min)	34
MoSSe/Co_3O_4 (0.2 g L^{-1})	Solvothermal Xenon lamp (300 W)	Tetracycline (10 mg L^{-1})	UV-VIS: 94% (90 min)	30
$Co_3O_4/MoS_2/SrTiO_3$	Wet impregnation Halogen lamp (500 W)	Methylene blue (100 mg L^{-1})	UV-VIS: 95% (100 min)	45
$Co_3O_4/CuBi_2O_4/SmVO_4$ (0.3 g L^{-1})	Mixing & calcination Xenon lamp (300 W)	Carbamazepine (10 mg L^{-1})	UV-VIS: 76% (300 min)	46
$Fe_3O_4/Co_3O_4/TiO_2$ (1 g L^{-1})	Sol–gel Natural sunlight[a]	Tetracycline (10 mg L^{-1})	UV-VIS: 100% (150 min) TOC: 100% (240 min)	47
Straddling and S-scheme composite				
$CeO_2/Co_3O_4/Ag/Ag_3PO_4$ (1 g L^{-1})	Electrospining & impregnation LED light[a]	Methylene blue (10 mg L^{-1})	UV-VIS: 93% (80 min)	48
Magnetic composite				
$ZnCo_2O_4/Co_3O_4$ (0.52 g L^{-1})	Green synthesis using *Stevia* extract & calcination Osram lamp (125 W)	Acid violet 7 (13 mg L^{-1})	UV-VIS: 93.5% (70 min)	49
Ag/Co_3O_4/$NiFe_2O_4$ (0.05 g L^{-1})	Multi-step precipitation LED light (1070 W m^{-2})	Tetracycline (10 mg L^{-1})	UV-VIS: 100% (250 min)	50
Co_3O_4/MK-30	Green synthesis using *Carissa edulis* extract & calcination Light source: N/A	Methylene blue (10 mg L^{-1})	UV-VIS: 98% (45 min)	51

[a] Light intensity is not reported in the referenced literature.

increased photocatalytic activity of PtO-doped Co_3O_4 was attributed to the ability of PtO to withdraw excited electrons from the conduction band of Co_3O_4, thereby facilitating the reduction of adsorbed O_2 into active radicals. Additionally, PtO was reported to establish a heterojunction electric field at the PtO/Co_3O_4 interface, effectively suppressing electron–hole recombination and significantly enhancing photocatalytic efficiency. However, no energy band determination of the synthesized materials was performed, rendering the inferences regarding the underlying photocatalytic mechanism inconclusive. The lack of post-reaction characterizations hinders a full assessment of PtO/Co_3O_4's long-term stability, and its practical applicability remains unclear due to the absence of testing under realistic water conditions.

5.2. Co_3O_4-based photocatalytic nanocomposites

Preparing photocatalytic composites offers several advantages over metal doping, making it a more effective and sustainable approach. Composite materials provide greater flexibility in design, allowing precise control over interfacial interactions, band alignment, and morphology. Different types of Co_3O_4-based photocatalytic composites were prepared in recent years for polluted water treatment.

Janani *et al.* prepared $Bi_6Cr_2O_{15}/Co_3O_4$ composite *via* a sonochemical precipitation method for the photocatalytic treatment of methylene blue[41] (Table 2). Similarly, Alhaddad *et al.* fabricated a Co_3O_4/TiO_2 composite using the impregnation method with a soft template for the treatment of the antibiotic ciprofloxacin.[42] Mohammadi *et al.* developed rGO-Co_3O_4/ZnO nanocomposite by through a two-step hydrothermal process for the degradation of parathion[28] (Fig. 3a). In a different investigation, Wang *et al.* synthesized Bi_2O_3/BN/Co_3O_4 photocatalyst *via* calcination and impregnation methods for the removal of norfloxacin. A common characteristic among these Co_3O_4-based photocatalytic systems is the formation of a straddling type-I heterojunction, which is generally considered the least effective due to its inefficient charge separation and high electron–hole recombination rates. In a straddling type-I heterojunction, the conduction and valence bands of one semiconductor are fully enclosed within the band structure of the second component, causing the accumulation of both photogenerated electrons and holes in the same material. This band alignment significantly increases the probability of electron–hole recombination, thereby limiting photocatalytic efficiency. Although comparing pollutant removal efficiencies across different systems is complicated by varying experimental conditions and target contaminants, a representative example is the Bi_2O_3/BN/Co_3O_4 composite.[29] As a straddling type-I heterojunction, it required 3 hours under high-intensity xenon lamp irradiation (500 W) and a large catalyst dosage (1 g L^{-1}) to

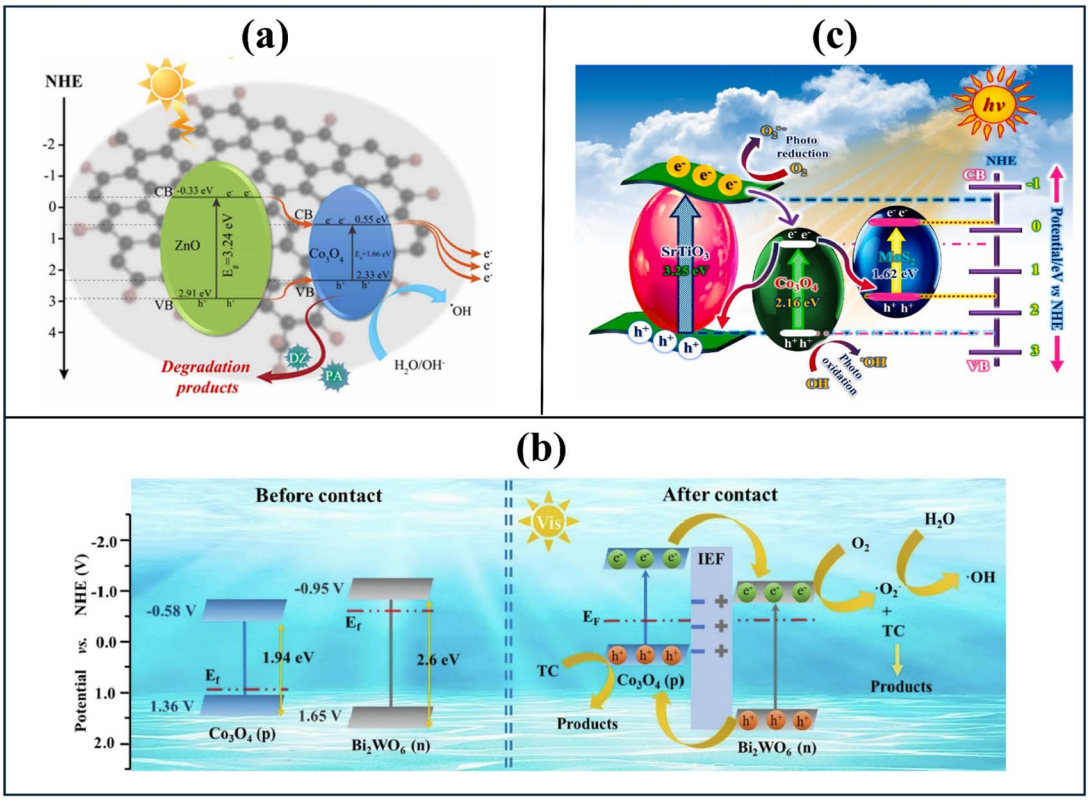

Fig. 3 Photocatalytic mechanism of the Co_3O_4 nanomaterial-based composites: Straddling type-I heterojunction system of rGO-Co_3O_4/ZnO composite[28] (a), type-II and p–n heterojunction system of $Co_3O_{4(QDs)}/Bi_2WO_6$ composite[35] (b), and dual Z-scheme system of Co_3O_4/MoS_2/$SrTiO_3$ composite[45] (c). Reprinted with permission from ref. 28 Copyright (2023), ref. 35 Copyright (2022), ref. 45 Copyright (2024) with permission from Elsevier.

degrade just 5 mg L^{-1} of antibiotics, illustrating the inherent limitations of this heterojunction design. Moreover, several critical limitations persist in these studies regarding the mechanistic understanding of photocatalysis. In the cases of $Bi_6Cr_2O_{15}/Co_3O_4$ and $Bi_2O_3/BN/Co_3O_4$, the electronic band structure and the primary active species involved in the photocatalysis were not determined. For the Co_3O_4/TiO_2 composite, no experimental evidence was provided to confirm the establishment of a p–n heterojunction or to elucidate the charge transmission pathways between the composite's constituents. Additionally, for rGO-Co_3O_4/ZnO system, no optimization studies were conducted to refine the synthesis process and identify the most effective composite configuration. Addressing these gaps through systematic experimental investigations will be vital for advancing the design and functionality of Co_3O_4 nanomaterial-based photocatalysts.

Compared to type-I heterojunctions, type-II and S-scheme heterojunctions enable more efficient utilization of visible light due to their favorable band alignment and charge transfer mechanisms. Zhang *et al.* prepared a Co_3O_4/Bi_2WO_6 composite by solvothermal and mixing techniques for the decomposition of tetracycline.[35] The optimized 10% Co_3O_4/Bi_2WO_6 composite demonstrated an 80% degradation efficiency for tetracycline (20 mg L^{-1}) within 20 minutes of visible light irradiation. The high photocatalytic activity was attributed to the construction of both p–n and type-II heterojunctions, which effectively suppressed charge carrier recombination (Fig. 3b). Especially, the degrading pathway of tetracycline and the generation of intermediates during photocatalysis were systematically investigated using advanced techniques, including three-dimensional excitation-emission matrix fluorescence and liquid chromatography/quadrupole time-of-flight mass spectrometry. Similarly, Tao *et al.* synthesized a heterogenous type-II red P/Co_3O_4 composite *via* hydrothermal and physical mixing methods for the degradation of malachite green.[43] The red P/Co_3O_4 photocatalytic system, at a dosage of 0.4 g L^{-1}, achieved 94% degradation of malachite green (20 mg L^{-1}) within just 20 minutes. However, a prolonged adsorption time of 30 minutes was required before the photocatalytic reaction commenced. A notable limitation of such type-II photocatalytic composites is that electrons and holes migrate to the conduction and valence bands with lower energy levels, thereby restricting their reactivity and ability to generate highly reactive radical species. In both the Co_3O_4/Bi_2WO_6 and red P/Co_3O_4 systems, photogenerated holes were transferred from the valence band of the secondary component to the less positive valence band of Co_3O_4. This hindered their capacity to oxidize water molecules and produce strong hydroxyl radicals, thereby limiting the overall oxidative potential of the system.

S-scheme heterojunctions facilitate enhanced redox capabilities by preserving highly energetic electrons and holes in spatially distinct locations, thereby improving charge carrier separation and promoting superior photocatalytic activity.[52] Several recent studies have explored Co_3O_4-based photocatalytic composites incorporating S-scheme charge transfer pathways. For instance, the research group of Armenia synthesized two S-scheme photocatalytic systems, Li_2MnO_3/Co_3O_4 and $CuCo_2O_4/Co_3O_4$, using a sol–gel approach with the F-127 surfactant as a soft template for the decomposition of tetracycline in water.[34,44] These nanocomposites were designed to integrate both S-scheme charge transfer and p–n junction formation between the p-type semiconductor Co_3O_4 and complementary n-type semiconductors, thereby elevating the separation of charge carriers and facilitating the generation of reactive radicals, such as superoxide radicals $^{\bullet}O_2^-$ and hydroxyl radicals $^{\bullet}OH$. However, further refinement in defining the energy band positions and band gaps of these systems is required to establish a more accurate understanding of photoinduced electron–hole mobility within the nanocomposites.

Ternary composites featuring a dual S-scheme charge transfer mechanism have demonstrated superior photocatalytic efficiency among Co_3O_4-based materials. In a representative study, Venkatesh G *et al.* prepared a $Co_3O_4/MoS_2/SrTiO_3$ composite *via* the wet impregnation method for the photocatalytic degradation of methylene blue dye.[45] The implementation of the double S-scheme mechanism facilitated the accumulation of electrons at the conduction bands of $SrTiO_3$ and MoS_2, while photogenerated holes remained in the valence band of Co_3O_4 (Fig. 3c). This efficient charge separation and transfer process enabled the generation of multiple reactive species, ultimately leading to the effective degradation of 95% of methylene blue (100 mg L^{-1}) within 100 min of light irradiation. Especially, the density functional theory method was employed to calculate the energy band structure and electronic density of states of the materials, thereby providing a robust theoretical foundation for elucidating the charge transfer process. The development of materials for environmental remediation should prioritize simplification, cost-effectiveness, and enhanced practical applicability. The synthesis of Co_3O_4-based quaternary composites through complex preparation routes should be avoided to facilitate scalable production. Most existing research has concentrated on the synthesis of Co_3O_4-based catalysts in powder form, which, despite offering high surface area, presents challenges in post-treatment separation and reuse. However, strategies to improve catalyst recovery, such as immobilizing the photocatalyst on floating carriers, polymeric membranes, or porous sponge-like substrates, remain underexplored. These approaches not only facilitate easy separation but also enhance the potential for continuous-flow or *in situ* water treatment systems, which are essential for practical and large-scale applications.

5.3. Magnetic Co_3O_4-based photocatalytic nanocomposites

Photocatalysts with facile recovery mechanisms are essential to ensuring sustainability, economic viability, and large-scale implementation. Heidari-Asil *et al.* synthesize nanoparticles $ZnCo_2O_4/Co_3O_4$ *via* a green synthesis approach using *Carissa edulis* extract,[49] enabling convenient recovery through an external magnetic field. By adjusting the concentration of Stevia extract, the glycoside content was effectively modified, significantly influencing the morphology and dimensions of the $ZnCo_2O_4/Co_3O_4$ nanostructures. The optimized nanocomposite exhibited high structural uniformity and achieved a degradation efficiency of 93.5% for acid violet 7 within 70 minutes of

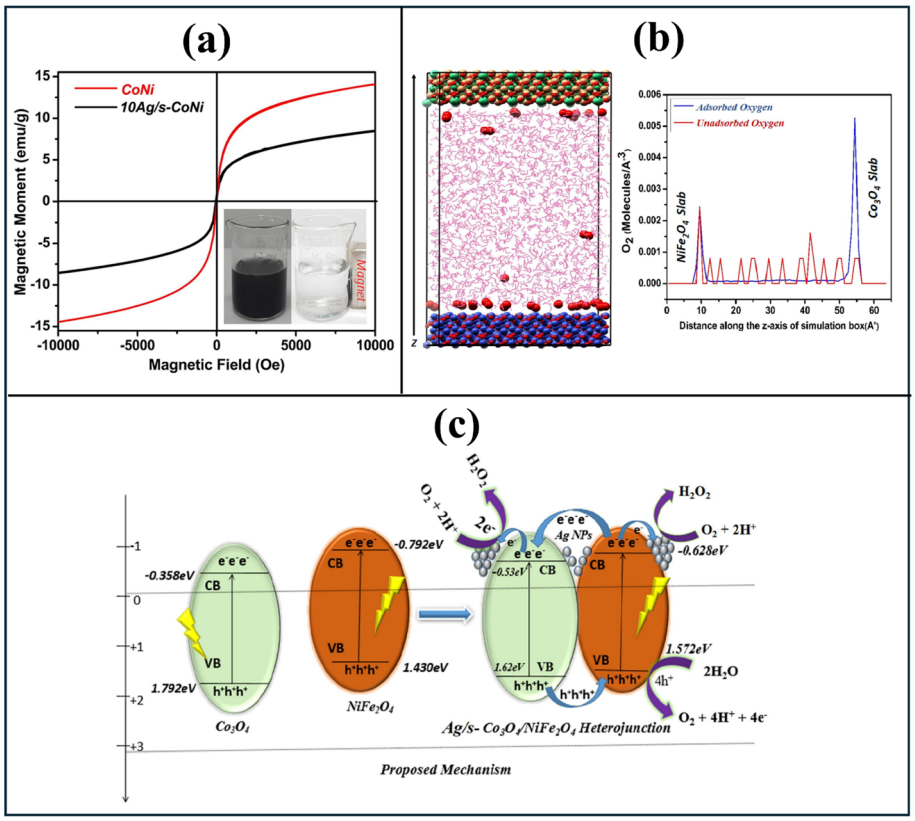

Fig. 4 Magnetization curve (a), molecular dynamics simulation for the adsorption of O_2 on two components of the composite (b), and photocatalytic mechanism of the Ag/Co_3O_4/$NiFe_2O_4$ photocatalytic system (c). Reprinted with permission from the ref. 50 Copyright (2022) with permission from Elsevier.

light exposure. The nanomaterial exhibits weak ferromagnetism at room temperature, with a remanence of 0.004 emu per g and coercivity of 48 Oe. This magnetic behavior enables rapid separation using an external magnet, facilitating catalyst recovery and contributing to a high photocatalytic efficiency after ten reuse cycles (93.5% in the first run and 81.7% after ten cycles). However, a notable limitation of this study is the absence of band gap measurements for the semiconductor components, which would provide greater insight into the photocatalytic mechanism of the composite.

Kumar *et al.* synthesized a magnetically recyclable composite by integrating polyhedral Co_3O_4 nanoparticles with the magnetic semiconductor $NiFe_2O_4$ for photocatalytic H_2O_2 production in tetracycline degradation[50] (Fig. 4a). Molecular dynamics simulations revealed that the adsorption capacity of O_2 on the Co_3O_4 surface was more than twice that observed on $NiFe_2O_4$, further contributing to the system's enhanced photocatalytic efficiency (Fig. 4b). Beyond the formation of an S-scheme heterojunction between Co_3O_4 and $NiFe_2O_4$, Ag doping played a pivotal role in enhancing H_2O_2 production. The presence of Ag nanoparticles significantly improved charge carrier dynamics by efficiently extracting photoexcited electrons from Co_3O_4 and $NiFe_2O_4$, thereby facilitating the direct reduction of O_2 molecules into H_2O_2 (Fig. 4c). The nanocomposite showed superparamagnetic behavior with a high saturation magnetization of approximately 14.2 emu per g, highlighting its potential for magnetically recoverable photocatalytic applications. The composite successfully achieved complete degradation of tetracycline (10 mg L^{-1}) within 250 minutes. However, its optimal performance at pH 3 presents a significant limitation, restricting its applicability for the rapid treatment of conventionally polluted water.

In a separate study, Co_3O_4 nanoparticles were dispersed onto magnetic montmorillonite K30 (MK-30) nanosheets *via* an ultrasonication-assisted method, demonstrating effective photocatalytic degradation of tetracycline.[51] In addition to imparting magnetic properties for rapid recovery, MK-30, with its negatively charged surface, was reported to facilitate the withdrawal of photogenerated positive holes, thereby enhancing charge carrier separation within the Co_3O_4/MK-30 composite and improving photocatalytic performance. Although the magnetic properties of Co_3O_4/MK-30 were not directly analyzed, the catalyst was easily recovered using an external magnetic field after each cycle, indicating magnetic separability. This enabled stable photocatalytic performance over five reuse cycles, highlighting its potential for efficient and reusable water treatment applications.

6. Co_3O_4 nanomaterial-based photocatalysts for oxidant activation in water treatment

Photocatalytic activation of oxidants is an advanced process that utilizes a photocatalyst to absorb light energy, initiating

redox reactions that activate oxidants such as hydrogen peroxide (H_2O_2), persulfates ($S_2O_8^{2-}$) and peroxymonosulfates (HSO_5^-). This activation leads to the generation of reactive oxygen species, which facilitate the decomposition of organic pollutants. Co_3O_4, a mixed-valence spinel oxide containing both Co^{2+} and Co^{3+}, serves as an efficient catalyst for oxidant activation through cyclic redox reactions, enabling effective electron transfer in oxidation–reduction processes even in the absence of light. However, photocatalytic activation of oxidants by Co_3O_4 has been reported to significantly enhance oxidation reactions due to the additional interaction of oxidants with photoexcited charge carriers, thereby improving overall catalytic efficiency.

In a study by Drummer *et al.* (2024), Co_3O_4 was synthesized *via* a green synthesis approach using spent coffee extract and employed for the activation of HSO_5^- in the treatment of tartrazine dye in water.[53] Under visible light, photoexcited electrons in Co_3O_4's conduction band reduced HSO_5^-, initiating a series of reactions that generate various reactive species, including $^{\bullet}O_2^-$, $^{\bullet}OH$, $^{\bullet}SO_4^-$, $^1O_2$, and $^{\bullet}SO_5^-$. Among these, sulfate and hydroxyl radicals identified as the primary active species responsible for the degradation of tartrazine (Fig. 5a). This photocatalytic activation enhanced the degradation rate constant by 37.6% compared to the reaction without light. The study further highlighted that the performance of the Co_3O_4/HSO_5^- system was highly dependent upon the type of light source used, including LED light, simulated sunlight, and natural sunlight. Minimal cobalt leaching (~0.0001%) suggests that Co_3O_4 activates HSO_5^- *via* a stable, heterogeneous mechanism for sulfate radical generation. Despite its promising photocatalytic performance, the study identified challenges related to the recovery and reuse of the nanomaterial, limiting its recyclability to only two cycles. To address this limitation, it is suggested that a growth template be employed during synthesis. To enhance structural stability and facilitate efficient retrieval of the nanocatalyst for repeated applications.

Similarly, nanospherical Co_3O_4 was integrated on laminated g-C_3N_4 to construct a heterostructured photocatalyst for the activation of HSO_5^- in the degradation of atrazine.[31] Density functional theory calculations revealed that the enhanced photocatalytic activity of Co_3O_4/g-C_3N_4 composite is primarily attributed to modifications in its electronic band structure, which promote efficient charge carrier separation and transfer. Upon the incorporation of Co_3O_4, the uniform distribution of Highest Occupied Molecular Orbital (HOMO) and Lowest Unoccupied Molecular Orbital (LUMO) within g-C_3N_4 was disrupted, thereby enhancing electron delocalization and mobility. Notably, for g-C_3N_4 to function effectively as a photocatalyst, its HOMO was required to be predominantly composed of the Co 3d state orbitals, serving as active sites for redox reactions. The activation of HSO_5^- in this system was predominantly driven by photoexcited electrons at conduction bands of g-C_3N_4 and g-C_3N_4 and by Co(II) (Fig. 5b). Scavenging experiments revealed that $^{\bullet}OH$, $^{\bullet}SO_4^-$, and e^- are the dominant reactive species

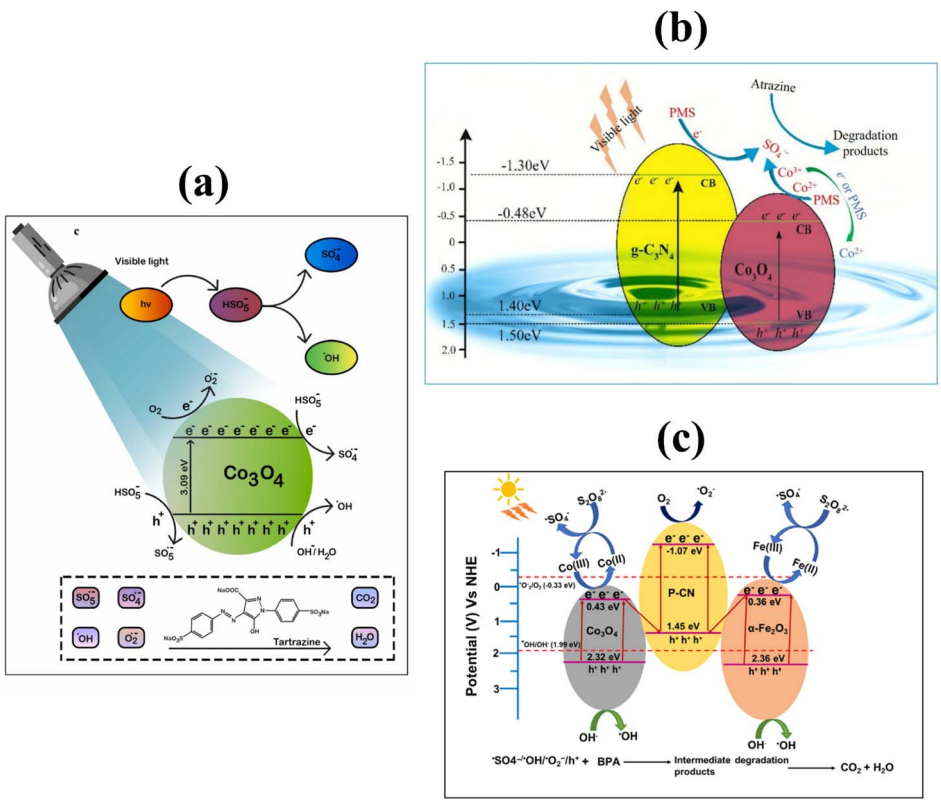

Fig. 5 Photocatalytic activation mechanism of oxidants by Co_3O_4 (ref. 53) (a), Co_3O_4/g-C_3N_4 (ref. 31) (b), and Co_3O_4@P–C_3N_4/α-Fe_2O_3 (ref. 54) (c). Reprinted with permission from the ref. 53 Copyright (2024), ref. 31 Copyright (2021), and ref. 54 Copyright (2024) with permission from Elsevier.

contributing the atrazine decomposition, whereas h^+ and $^{\bullet}O_2^-$ play relatively minor roles. The system achieved 79% degradation of atrazine (10 mg L^{-1}) within 35 minutes of light irradiation. The Co_3O_4/g-C_3N_4 catalyst demonstrated high stability, as confirmed by recycling tests for atrazine degradation, cobalt ion leaching assessments, and structural analyses *via* XRD and XPS.

In a different work, Rangaraj *et al.* fabricated a ternary composite by incorporating Co_3O_4 with Fe_2O_3 and P-doped g-C_3N_4 for the activation of persulfate in the treatment of bisphenol A.[54] The composite exhibited a low charge carrier recombination rate, ascribed to the formation of a double Z-scheme heterojunction, which effectively enhanced charge separation and transfer. Additionally, the composite demonstrated magnetic properties, facilitating its retrieval and reuse after catalytic reactions. Persulfate has been reported to react with Co(II), Fe(II), and photogenerated electrons in the conduction bands of the composite components, resulting in the generation of sulfate radicals (Fig. 5c). In this study, the synergistic action of reactive species, including h^+, $^{\bullet}OH$, $^{\bullet}SO_4^-$, facilitated the efficient degradation of bisphenol A (20 mg L^{-1}), achieving a removal efficiency of 90% within 90 minutes. However, the study did not explore the optimal composition ratios of the individual components during the synthesis process. Furthermore, it did not include an analysis of the energy band structure or investigate the potential shifts in band alignment resulting from the combination of p- and n-type semiconductors within the composite system.

From the reviewed studies, persulfate and peroxymonosulfate have been commonly selected as oxidants activated by Co_3O_4-based photocatalysts for advanced water treatment. This preference is likely due to their ability to generate various reactive species, particularly strong radicals such as $^{\bullet}SO_4^-$ and $^{\bullet}OH$, which exert synergistic effects in the degradation of recalcitrant pollutants. Among the two, persulfate has been recommended as the more effective oxidant. This is because PS is primarily reduced by photoinduced electrons from the catalyst to produce sulfate radicals, whereas PMS can also be oxidized by photogenerated holes to form HSO_5^-, a weaker oxidant with lower redox potential. Moreover, prolonged exposure to strong oxidants and reactive species may degrade Co_3O_4 structure and limit reusability. Therefore, comprehensive stability assessments, including recycling tests, leaching analysis, and post-reaction characterizations, are essential to ensure practical applicability and sustained performance under real-world conditions.

7. Computational applications

Computational approaches, particularly Density Functional Theory (DFT), play a pivotal role in photocatalysis research by providing atomic-scale insights into the electronic, structural, and energetic properties of photocatalytic materials. However, studies focusing on Co_3O_4-based nanomaterials for photocatalytic water treatment have rarely integrated computational methods with experimental techniques to optimize photocatalyst design, explore band structure and density of states (DOS), or elucidate photocatalytic reaction pathways.

In the study conducted by Mohammadi *et al.*,[55] GO/Co_3O_4/ZnO photocatalytic nanocomposite was employed for the degradation of the insecticide parathion. The response surface methodology employing a quadratic polynomial model was applied to design the experiments and optimize the photocatalytic performance by evaluating key operational parameters. Through statistical analysis, the optimal conditions were identified as a pH of 12, parathion concentration of 5 mg L^{-1}, photocatalyst dosage of 0.12 g, reaction duration of 2.3 hours, and light intensity of 14 W cm^{-2}. In a separate study, Chen *et al.* applied DFT to model the crystal structure, simulate the energy band structure, and analyze the density of states of Au/Co_3O_4/Bi_2MoO_6 composite used for photocatalytic decomposition of methyl orange dye.[56] The computational simulations revealed that incorporating Co_3O_4 into the composite significantly

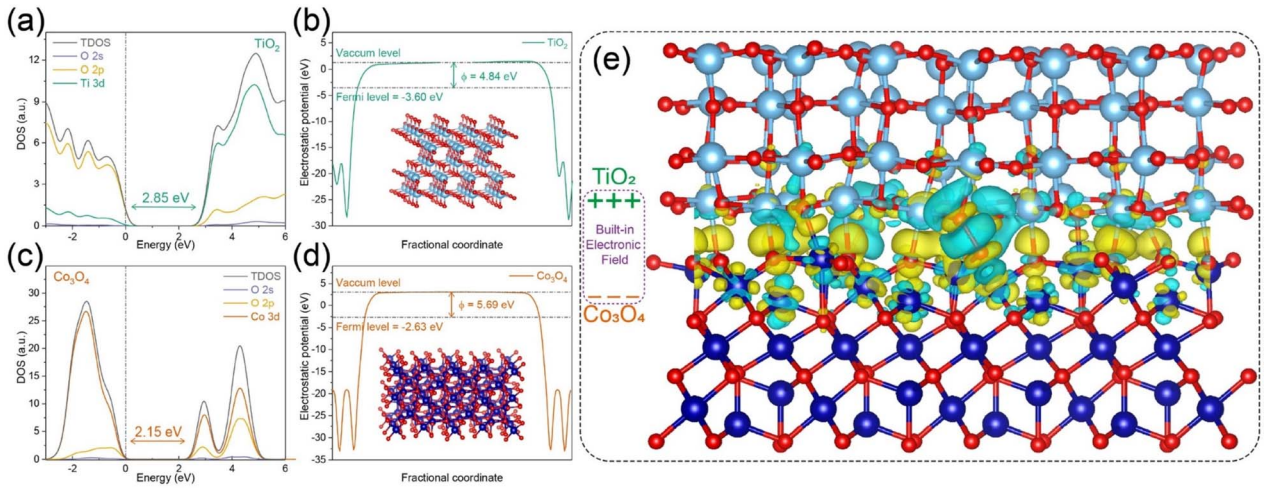

Fig. 6 The calculated density of states for (a) TiO_2 and (c) Co_3O_4, alongside the electrostatic potential for (b) TiO_2 and (d) Co_3O_4. Panel (e) depicts the built-in electric field formed at the TiO_2/Co_3O_4 interface. Reprinted with permission from the ref. 58, Copyright (2020) with permission from Elsevier.

reduced the band gap (1.84 eV for Co_3O_4/Bi_2MoO_6 compared to 2.72 eV for Bi_2MoO_6) and enhanced the O 2p and Co 3d electron density near the Fermi level, thereby promoting charge carrier transfer and improving photocatalytic efficiency. Furthermore, Guo *et al.* synthesized a visible light-activated Co_3O_4/Bi_2MoO_6 nanocomposite for peroxymonosulfate-assisted degradation of the antibiotic norfloxacin.[57] DFT calculations were successfully employed to elucidate the photocatalytic mechanism, revealing the energy band structure and confirming the formation of a p–n heterojunction between Co_3O_4 and Bi_2MoO_6, which enhanced charge separation and transfer. Similarly, Y. Wang *et al.* incorporated Co_3O_4 nanodots onto TiO_2 nanosheets to fabricate Co_3O_4/TiO_2 nanocomposite for the photocatalytic degradation of antibiotic enrofloxacin.[58] DFT simulations were utilized to predict the energy band structure and electron density distribution. TiO_2 exhibited a lower Fermi level and work function compared to Co_3O_4, indicating a directional electron flow from TiO_2 to Co_3O_4 at the interface (Fig. 6). Additionally, the density of states analysis revealed that interfacial oxygen atoms contributed to heterojunction formation, thereby facilitating charge transfer across the interface. This charge redistribution led to the alignment of Fermi levels between the two components, resulting in the formation of a built-in electric field that enhanced electron–hole separation and migration, ultimately improving the photocatalytic performance.

8. Future perspectives and challenges

The research on Co_3O_4 nanomaterials for water treatment continues to be a highly promising field, offering substantial opportunities for further exploration. To achieve breakthroughs in the synthesis of Co_3O_4 nanostructures with novel morphologies and advanced electronic and optical properties, state-of-the-art synthesis strategies, such as template-assisted pyrolysis, atomic layer deposition, and nanoconfinement techniques, should be prioritized to precisely tailor the structural and physicochemical characteristics of Co_3O_4.

MOF-derived Co_3O_4 nanomaterials present a distinctive platform for designing hierarchical nanostructures with high surface area, tunable porosity, and controllable morphology. Despite their promising photocatalytic activity, challenges related to inefficient charge carrier separation persist due to intrinsic band structure limitations. Therefore, future research should focus on band gap engineering through cation doping, defect modulation, and oxygen vacancy engineering to enhance light absorption, facilitate charge movement, and prolong charge carrier lifetimes.

The capacity of Co_3O_4 to activate oxidants should be further explored to maximize its application for water purification. Key research directions should include mechanistic elucidation of oxidation pathways, optimization of oxidant-to-photocatalyst ratios, and development of light-assisted Fenton-like and sulfate radical-based oxidation systems. Prolonged exposure to oxidants may degrade Co_3O_4 structure and limit reusability, highlighting the need for thorough stability assessments to ensure long-term applicability.

Prolonged photocatalytic reactions can lead to aggregation, cobalt ion leaching, structural degradation, and challenges in catalyst recovery, all of which hinder the practical application of Co_3O_4 nanomaterials. Core-shell coating is a solution to enhance the structural integrity and chemical stability of Co_3O_4. Immobilization of Co_3O_4 nanomaterials on substrates such as membranes, glass, ceramics, or polymer films allows convenient recovery without compromising photocatalytic efficiency. Additionally, integrating Co_3O_4 with other magnetic semiconductors to develop S-scheme heterojunction nanocomposites should be a priority, as the S-scheme charge transfer mechanism has demonstrated superior photocatalytic performance while maintaining facile recovery *via* magnetic separation.

To align with environmental sustainability goals, research efforts should focus on eco-friendly synthesis methodologies, such as bio-derived precursors, solvent-free synthesis, and low-temperature calcination processes. Utilizing biomass-derived templates or waste-derived metal sources for precursors could reduce the environmental impact and improve the economic feasibility of Co_3O_4 photocatalysts.

To enable commercial application of Co_3O_4-based photocatalysts, future studies must aim for high degradation efficiencies within short irradiation times, even under visible or solar light. In addition, consistent performance over multiple reuse cycles and in complex real wastewater matrices must be demonstrated. Standardization of photocatalytic metrics such as apparent quantum yield and total organic carbon removal will allow meaningful comparison between systems. Furthermore, low-cost, scalable synthesis, combined with magnetic recovery and low catalyst dosage, will be essential for reducing operational costs and enabling large-scale implementation.

A comprehensive understanding of the photocatalytic mechanisms in Co_3O_4-based systems necessitates the integration of cutting-edge experimental and computational techniques. For example, *Operando* X-ray photoelectron spectroscopy is useful to monitor band edge shifts under real–time reaction conditions. Hard X-ray photoelectron spectroscopy is effective for probing buried interfaces in heterojunctions. Moreover, frequency-resolved Mott–Schottky analysis is very helpful for precise determination of band edge positions and charge carrier dynamics. Beside the experimental methods, computational techniques like density functional theory calculations and molecular dynamics simulations should be conducted simultaneously to predict electronic structures, charge transport mechanisms, and band alignment and verify the experimental results.

9. Conclusions

Despite extensive research on Co_3O_4 nanomaterial-based photocatalysts, a critical gap remains in comprehensive reviews that consolidate recent advancements in their application for water treatment. This review provided an in-depth analysis of key photocatalytic mechanisms, inherent advantages, existing limitations, and prospective research directions of Co_3O_4 nanomaterial-based photocatalysts for water treatment in the

recent five years. Various Co_3O_4 nanostructures have been synthesized through diverse methodologies for their implementation as photocatalysts in wastewater treatment. Furthermore, extensive efforts have been dedicated to modifying Co_3O_4 and integrating it with other functional materials to enhance charge carrier separation, improve degradation efficiency, and facilitate catalyst recovery for practical applications. However, a significant number of studies have yet to elucidate the precise catalytic mechanisms and the roles of reactive oxygen species in degradation processes.

Future perspectives and challenges on the Co_3O_4 nanomaterial-based photocatalysts for water treatment were proposed. To enhance Co_3O_4 nanomaterial's performance, advanced synthesis techniques should be applied for precise control over its structure and properties. MOF-derived Co_3O_4 offers high surface area and tunable porosity, but improved band gap engineering *via* doping, defect modulation, and oxygen vacancy control is needed for better charge separation. Further studies should optimize Co_3O_4 nanomaterial's role in oxidant activation, including light-assisted Fenton-like and sulfate radical-based systems. Challenges like aggregation, leaching, and recovery must be addressed through core–shell coatings, immobilization, and magnetic S-scheme heterojunctions. Sustainable synthesis approaches should improve environmental and economic viability. Finally, integrating advanced spectroscopic techniques with computational modeling is essential for understanding charge transfer mechanisms. Addressing these challenges will optimize Co_3O_4 nanomaterial-based photocatalysts for scalable and sustainable water treatment solutions.

Data availability

No primary research results, software or code have been included and no new data were generated or analysed as part of this review.

Author contributions

Van Dien Dang: writing (original draft), investigation, visualization. Nguyen Thi Hong Nhung: writing (original draft), Iqra Rabani: conceptualization, writing (original draft), Nguyen Tien Tran: writing (original draft), Bui Thi Phuong Thuy: writing (original draft), Hai Bang Truong: writing (review& editing), project administration, supervision, validation.

Conflicts of interest

The authors declare that they have no known competing financial interests or personal relationships that could have appeared to influence the work reported in this paper.

References

1 A. Boretti and L. Rosa, *npj Clean Water*, 2019, **2**, 1–6.
2 I. Rabani, M. S. Tahir, F. Afzal, H. B. Truong, M. Kim and Y.-S. Seo, *J. Environ. Chem. Eng.*, 2023, **11**, 109235.
3 S. K. Ray, H. B. Truong, Z. Arshad, H. S. Shin and J. Hur, *Membr. Water Treat.*, 2020, **11**, 257–274.
4 H. Bang Truong, X. Cuong Nguyen and J. Hur, *J. Environ. Manage.*, 2023, **345**, 118895.
5 Y. Yang, X. Li, C. Zhou, W. Xiong, G. Zeng, D. Huang, C. Zhang, W. Wang, B. Song, X. Tang, X. Li and H. Guo, *Water Res.*, 2020, **184**, 116200.
6 M. Ismael, *J. Alloys Compd.*, 2020, **846**, 156446.
7 C. Prasad, H. Tang and I. Bahadur, *J. Mol. Liq.*, 2019, **281**, 634–654.
8 Z. Yu, F. Li and Q. Xiang, *J. Mater. Sci. Technol.*, 2024, **175**, 244–257.
9 H. H. Do, Q. Van Le and H. B. Truong, *Korean J. Chem. Eng.*, 2024, **41**, 2227–2237.
10 R. Subagyo, A. Yudhowijoyo, N. A. Sholeha, S. S. Hutagalung, D. Prasetyoko, M. D. Birowosuto, A. Arramel, J. Jiang and Y. Kusumawati, *J. Colloid Interface Sci.*, 2023, **650**, 1550–1590.
11 H. H. Do and H. B. Truong, *Beilstein J. Nanotechnol.*, 2023, **14**, 904–911.
12 J. Ma, H. Wei, Y. Liu, X. Ren, Y. Li, F. Wang, X. Han, E. Xu, X. Cao, G. Wang, F. Ren and S. Wei, *Int. J. Hydrogen Energy*, 2020, **45**, 21205–21220.
13 H. B. Truong, B. T. Huy, S. K. Ray, Y.-I. Lee, J. Cho and J. Hur, *Chem. Eng. J.*, 2020, **399**, 125733.
14 A. M. Nasir, J. Jaafar, F. Aziz, N. Yusof, W. N. W. Salleh, A. F. Ismail and M. Aziz, *J. Water Process Eng.*, 2020, **36**, 101300.
15 H. B. Truong, T. T. L. Doan, N. T. Hoang, N. Van Tam, M. K. Nguyen, L. G. Trung, J. S. Gwag and N. T. Tran, *J. Environ. Sci.*, 2024, **139**, 569–588.
16 F. Lu and D. Astruc, *Coord. Chem. Rev.*, 2018, **356**, 147–164.
17 D. Zhou, J. Yu, J. Tang, X. Y. Li and P. Ou, *Adv. Energy Mater.*, 2025, **15**, 2404007.
18 A. Matsuda, R. Yamauchi, D. Shiojiri, G. Tan, S. Kaneko and M. Yoshimoto, *Appl. Surf. Sci.*, 2015, **349**, 78–82.
19 S. Vladimirova, V. Krivetskiy, M. Rumyantseva, A. Gaskov, N. Mordvinova, O. Lebedev, M. Martyshov and P. Forsh, *Sensors*, 2017, **17**, 2216.
20 N. Bayati-Komitaki, S. H. Ganduh, A. H. Alzaidy and M. Salavati-Niasari, *Biomed. Pharmacother.*, 2024, **180**, 117457.
21 O. Brummel and J. Libuda, *Catal. Letters*, 2020, **150**, 1546–1560.
22 V. Mandić, S. Kurajica, M. Plodinec and I. Panžić, *Catalysts*, 2022, **12**, 1162.
23 G. Ziwa, R. Crane and K. A. Hudson-Edwards, *Minerals*, 2020, **11**, 22.
24 N. R. Khalid, A. Gull, F. Ali, M. B. Tahir, T. Iqbal, M. Rafique, M. A. Assiri, M. Imran and M. Alzaid, *Ceram. Int.*, 2022, **48**, 32009–32021.
25 L. Zhang, H. Li, K. Li, L. Li, J. Wei, L. Feng and Q. Fu, *J. Alloys Compd.*, 2016, **680**, 146–154.
26 S. Kumar, G. Kaur, M. Rawat, Y. F. Tsang, K. Y. Lin and K. H. Kim, *J. Clean. Prod.*, 2022, **361**, 132242.
27 P. D. Sarvalkar, A. S. Jamadar, S. S. kakade, A. B. Magdum, P. K. Pawar, J. B. Yadav, M. S. Nimbalkar, N. R. Prasad,

A. A. Ramteke and K. K. K. Sharma, *Results Eng*, 2024, **22**, 102094.
28 A. Mohammadi, H. Mirhosseini, A. Hekmatiyan, L. Abdolahi, F. Mehrabi and M. Shahmirzaei, *J. Environ. Chem. Eng.*, 2023, **11**, 110912.
29 N. Wang, W. Wang, D. Qi, G. Kang, B. Wang, H. Zhang, J. Ruan, R. Lei, Z. Zhang, S. Zhang and H. Zhou, *Chemosphere*, 2024, **352**, 141481.
30 X. Xiong, J. Zhang, C. Chen, S. Yang, J. Lin, J. Xi and Z. Kong, *J. Alloys Compd.*, 2022, **926**, 166863.
31 Q. Yang, J. An, Z. Xu, S. Liang and H. Wang, *Colloids Surf., A*, 2021, **614**, 126161.
32 S. Dhiman and B. Gupta, *Environ. Technol. Innov.*, 2021, **23**, 101765.
33 J. Yang, M. Wang, S. Zhao, Y. Liu, W. Zhang, B. Wu and Q. Liu, *Int. J. Hydrogen Energy*, 2019, **44**, 870–879.
34 S. H. Almenia, A. A. Ismail, K. A. Alzahrani and M. Aljahdali, *J. Photochem. Photobiol. A Chem.*, 2023, **438**, 114507.
35 X. Zhang, H. Zhang, J. Yu, Z. Wu and Q. Zhou, *Appl. Surf. Sci.*, 2022, **585**, 152547.
36 N. Imanuella, K. H. Ng, L. A. Tuyen and N. Q. Hung, *Appl. Catal. B: Environ*, 2024, **358**, 124401.
37 S. Adhikari, S. Mandal and D. H. Kim, *Appl. Surf. Sci.*, 2024, **653**, 159374.
38 N. R. Khalid, A. Gull, F. Ali, M. B. Tahir, T. Iqbal, M. Rafique, M. A. Assiri, M. Imran and M. Alzaid, *Ceram. Int.*, 2022, **48**, 32009–32021.
39 S. P. Keerthana, R. Yuvakkumar, P. S. Kumar, G. Ravi, D. V. N. Vo and D. Velauthapillai, *Chemosphere*, 2021, **277**, 130325.
40 R. M. Mohamed, A. A. Ismail, A. S. Basaleh and H. A. Bawazir, *J. Photochem. Photobiol. A Chem.*, 2022, **428**, 113859.
41 B. Janani, A. Syed, H. A. AL-Shwaiman, M. M. Alkhulaifi, A. M. Elgorban and S. S. Khan, *Colloids Surf., A*, 2021, **622**, 126671.
42 M. Alhaddad, A. A. Ismail, Y. G. Alghamdi, N. D. Al-Khathami and R. M. Mohamed, *Opt. Mater.*, 2022, **131**, 112643.
43 J. Tao, M. Zhang, X. Gao, H. Zhao, Z. Ren, D. Li, J. Li, R. Zhang, Y. Liu and Y. Zhai, *Mater. Chem. Phys.*, 2020, **240**, 122185.
44 S. H. Almenia, A. A. Ismail, K. A. Alzahrani and M. Aljahdali, *J. Alloys Compd.*, 2023, **953**, 170127.
45 G. Venkatesh, P. D. Shobana, N. Elavarasan, A. Rajesh, S. Senthilnathan and V. Vighesh, *Mater. Sci. Semicond. Process.*, 2024, **169**, 107909.
46 P. J. Mafa, M. E. Malefane, A. O. Idris, B. B. Mamba, D. Liu, J. Gui and A. T. Kuvarega, *J. Colloid Interface Sci.*, 2021, **603**, 666–684.
47 M. M. Abutalib, H. M. Alghamdi, A. Rajeh, O. Nur, A. M. Hezma and M. A. Mannaa, *J. Mater. Res. Technol.*, 2022, **20**, 1043–1056.
48 M. M. Sabzehmeidani, H. Karimi and M. Ghaedi, *Mater. Res. Bull.*, 2022, **147**, 111629.
49 S. A. Heidari-Asil, S. Zinatloo-Ajabshir, H. A. Alshamsi, A. Al-Nayili, Q. A. Yousif and M. Salavati-Niasari, *Int. J. Hydrogen Energy*, 2022, **47**, 16852–16861.
50 U. Kumar, J. Kuntail, A. Kumar, R. Prakash, M. R. Pai and I. Sinha, *Appl. Surf. Sci.*, 2022, **589**, 153013.
51 T. Chellapandi, S. M. Roopan and G. Madhumitha, *Environ. Res.*, 2023, **219**, 115052.
52 F. Li, Z. Fang, Z. Xu and Q. Xiang, *Energy Environ. Sci.*, 2024, **17**, 497–509.
53 S. Drummer, O. Mkhari and M. Chowdhury, *Next Nanotechnol.*, 2024, **6**, 100069.
54 V. M. Rangaraj, S. Devaraju, T. G. Reddy, H. Zafar, D. H. Anjum and V. Mittal, *Mater. Res. Bull.*, 2024, **179**, 112925.
55 A. Mohammadi, H. Mirhosseini, A. Hekmatiyan, L. Abdolahi, F. Mehrabi and M. Shahmirzaei, *J. Environ. Chem. Eng.*, 2023, **11**, 110912.
56 Q. Chen, B. Miao, Y. Hao, H. Wang and Q. Chen, *J. Alloys Compd.*, 2022, **902**, 163804.
57 J. Guo, C. H. Shen, J. Sun, X. J. Xu, X. Y. Li, Z. H. Fei, Z. T. Liu and X. J. Wen, *Sep. Purif. Technol.*, 2021, **259**, 118109.
58 Y. Wang, C. Zhu, G. Zuo, Y. Guo, W. Xiao, Y. Dai, J. Kong, X. Xu, Y. Zhou, A. Xie, C. Sun and Q. Xian, *Appl. Catal. B: Environ*, 2020, **278**, 119298.